RASĀYAN *J. Chem.*
Vol. 16 | No. 4 |2345-2352| October - December | 2023
ISSN: 0974-1496 | e-ISSN: 0976-0083 | CODEN: RJCABP
http://www.rasayanjournal.com
http://www.rasayanjournal.co.in

MODIFICATION OF NATURAL ZEOLITE FROM BOGOR FOR HYDROGEN STORAGE

Silvester Tursiloadi[1,✉], Aan Wahyuni[2], Lenny Marlinda[2], Muhammad Safaat[1], Latifa Hauli[1], Wiyanti Fransisca Manulang[1,4], Amalia Kurnia Amin[1], Deni Shidqi Khaerudini[3] and Muhammad Al Muttaqii[1]

[1]Research Center for Chemistry, National Research and Innovation Agency of Indonesia (BRIN), Kawasan Puspiptek, Serpong, Tangerang Selatan, Banten, Indonesia, 15314
[2]Department of Chemistry, Faculty of Science and Technology, University of Jambi University, Indonesia, 36361
[3]Research Center for Advanced Materials, National Research and Innovation Agency of Indonesia (BRIN), Kawasan Puspiptek, Serpong, Tangerang Selatan, Banten, Indonesia, 15314
[4]Chemical Engineering Department, Faculty of Engineering, Widya Mandala Surabaya Catholic University, Surabaya 60112, Indonesia
✉Corresponding Author: silv001@brin.go.id

ABSTRACT

Using hydrogen as an energy source still needs improvement, especially in storing hydrogen. Zeolite is a material with a large surface area and high porosity. When NaOH is added to natural zeolite Bogor, it breaks down into microporous (2 nm) and mesoporous (2–50 nm) zeolite. This zeolite with two different sizes of pores is called hierarchical zeolite. The wet impregnation method mixed Ni with zeolite using $Ni(NO_3).6H_2O$, which lets H_2 adsorb through a spillover mechanism. The characterization of the materials was analyzed using a Particle Size Analyzer (PSA), X-ray diffraction (XRD), and a Surface Area Analyzer (SAA). Temperature-programmed desorption-H_2 (TPD-H_2) determined the adsorption capacity for H_2 gas. The adsorption capacity of H_2 for different adsorption times (30, 45, 60, 75, and 90 min) was 0.1745, 0.3620, 0.7624, 0.2333, and 0.1802wt%, respectively. The highest adsorption capacity is 0.7624 wt.% with 60 min of adsorption time. When Ni metal was added to zeolite, it blocked or clogged the pores, lowering the adsorption capacity to 0.1405 wt.% and making H_2 adsorption less efficient.

Keywords: Natural Zeolite, Desilication, Hydrogen Storage.

RASĀYAN*J. Chem.*, Vol. 16, No. 4, 2023

INTRODUCTION

More than 80% of the world's energy needs are met using fossil energy sources (petroleum, natural gas, and coal).[1] If the use of fossil fuels remains the same, CO_2 emissions will increase from 32.3 billion metric tons in 2012 to 35.6 billion metric tons in 2020.[2] Hydrogen energy is an alternative energy source that has the potential to replace fossil fuels because hydrogen is the most abundant element in the universe and on the earth's surface (after oxygen and silicon). Hydrogen has a gravimetric energy density of 33.3 kWh/kg and an energy content 2.75 times greater than that of fossil fuels.[3] Hydrogen is a good energy source for the environment because it can be burned with oxygen to make energy and water vapor.[4] One of the biggest obstacles to realizing a hydrogen economy is how to store hydrogen more effectively and safely. High-pressure and cryogenic tanks are not yet promising from a safety point of view, and there is a risk of leakage.[5] Hydrogen stored in hydrides is safer, but the process of getting the hydrogen out requires high temperatures.[6] One of the safest and most efficient hydrogen storage methods is the adsorption method on porous materials.[7] Hydrogen can be stored in porous materials through a process called physisorption. This is the mechanism by which hydrogen molecules stick to the surface of porous materials. This happens in a reversible way and at a fast rate, so the process of hydrogen adsorption and desorption happens quickly.[8] Zeolite is a highly regular alumina silicate mineral with interconnected cavities in all directions, which causes a large surface area, so it has the potential to be used as an adsorbent, catalyst, and support. To make zeolite with the right properties for hydrogen adsorption, it had to be activated and changed. The activation of zeolite with NaOH can increase the surface area of zeolite from 19 m^2/g to 129 m^2/g.[9] Treatment of

http://doi.org/10.31788/RJC.2023.1648306

zeolite with NaOH is called desilication and produces hierarchical porous (microporous and mesoporous) zeolites. The addition of an active metal to the support can increase the hydrogen storage effect through a spillover mechanism, one of which is by adding transition metals such as Ni. Liao *et al*. (2017) reported that impregnating CeO^{2-} with Ni metal increased the value of H_2 adsorption from 7.87 mol/g to 65.55 mol/g.[10] This research was conducted to modify natural zeolite by alkaline treatment (desilication) using NaOH into hierarchical zeolite impregnated with Ni metal to increase the adsorption capacity of hydrogen. The effect of adsorption time on the ability of H_2 to be absorbed was also investigated.

EXPERIMENTAL

Materials

Bogor natural zeolite was supplied by PT. Astraindo, Bogor, Indonesia. NaOH, NH_4Cl, $AgNO_3$, and $Ni(NO_3)_2.6H_2O$ were obtained from Merck.

Preparation of Hierarchical Zeolite

Natural zeolite was crushed in a mortar and sieved using a sieve shaker to divide the particles. A 250-mL zirconia grinding jar was used in a Retsch PM200 ball mill to grind zeolite. A 2:4:4 ratio of zirconium oxide balls (5, 10, and 15 mm) was employed as grinding media. The rotational speed was 400 rpm, and the mass ratio of powder to ball was 10:1. Zeolite was ground for 1 h, with a 10-minute break between each grinding session. 400 mL of NaOH 0,1 M was combined with 20 g of natural zeolite, and the mixture was agitated for 2 h at 75°C. After filtering, the resultant zeolite was washed with distilled water to pH 7 and dried for 12 h at 110°C. After that, the zeolite was combined with 150 mL of NH_4Cl 1 M and refluxed for 8 h at 80 °C. After filtering and rinsing with distilled water until clear of Cl-ions, the mixture was dried for 12 h at 110°C and then calcined for 4 h at 500°C. This approach makes use of earlier studies.[11–12] Using $Ni(NO_3)2.6H_2O$ as a starting material, a wet impregnation method added 5 wt% Ni to the zeolite, followed by calcination at 500 °C for 2.5 h and reduction by H_2 at 500 °C for 4 h.

Characterization of Zeolite

To confirm the difference in particle size between the pre-milling and post-milling phases of zeolite, a PSA CILAS 1190 Liquid, 0.04 m–2500 m, was used. Using Cu-K as the radiation source, X-ray diffraction (XRD PANalyical Aeris) was used to determine the crystalline phase and crystallinity of the zeolite. The Surface Area Analyzer (Micromeritics TriStar II 3020) was used to find the specific surface area, the distribution of pore sizes, and the volume of the pores. These were found using the Brunauer-Emmett-Teller (BET) and Barrett-Joyner-Halenda (BJH). For 2 h, the sample was degassed at 200°C.

H_2 Adsorption Capacity

Temperature-programmed desorption (H_2-TPD) (Micromeritics ChemiSorbs 2750) was used to adsorb H_2 at room temperature and pressure for different amounts of time (30, 45, 60, 75, and 90 min). The sample was heated for 1 h under He (inert) at 350°C. After being cooled to room temperature, the sample was run through a combination of H_2/Ar gas for 30, 45, 60, 75, and 90 min at a 40 mL/min flow rate. After that, it was flushed with Ar for 30 min at the same temperature. 800 °C was then reached (at a rate of 10 °C per min). On the QMS detector, the desorbed H_2 was recorded as a function of time and temperature. The entire peak area under the desorption profile was used to determine the H_2 uptake.

RESULTS AND DISCUSSION

Characterization of Zeolite

A PSA analysis confirms the difference in particle size before and after milling, as Table-1 illustrates.

Table-1: PSA Analysis Results

Sample	Particle size distribution (μm)			Mean diameter (μm)
	D_{10}	D_{50}	D_{90}	
Before milling	1.69	9.29	37.97	15.16
After milling	1.41	4.99	17.10	7.46

Table-1 shows that there is a decrease in the average particle size after milling from 15.16 to 7.46 μm. The decrease in particle size occurs due to the collision between the zeolite particles and the grinding balls, which causes the samples to be split into smaller sizes. The values of D_{10}, D_{50}, and D_{90} express the particle

size distribution. Table-1 shows the decreasing values of D_{10}, D_{50}, and D_{90} after milling. These results indicate that milling for 1 h can reduce the particle size to about 2 times the initial particle size. Milling also makes the size distribution of the particles more even, in addition to reducing the size of the particles.[13] Milling conditions, such as rotational speed, ball-to-powder ratio (BPR), and milling time, also play an important role. 10.5- and 3-mm zirconia balls as grinding media with a ratio of 4:3:3, BPR 10:1, and milling for 1 h are proven to reduce the particle size up to 2 times the initial size. The selection of zirconia balls as a grinding medium is because, in the milling process, the grinding media must have a higher hardness level than the sample. Zirconia has a higher hardness level than zeolite, which is >9 mohs (LSP Industrial Ceramic, 2017), while zeolite has a hardness of 4.5 mohs (Minerals Education Coalition, 2022). XRD investigation determines the phase and crystallinity of the materials. Based on JCPDS No. 29-1257 14-17 for Mordenite for more information, Fig.-1 illustrates that Bogor zeolite is a zeolite with a clinoptilolite and mordenite framework. The diffraction peak appears at 13.5°, 19.7°, 25.7°, and 27.6°, corresponding to the (111), (330), (202), and (511) planes. Based on JCPDS No. 25-1349 18-21 for clinoptilolite, which corresponds to (020), (200), (111), (131), and (222) planes and has a diffraction peak at 9.72°, 11.14°, 17.32°, 22.27°, and 26.57°. According to JCPDS No. 47-1049 [22-23], the impregnation of Ni metal results in the formation of additional diffraction peaks at 37.15°, 43.23°, and 62.83°. These peaks correspond to the (111), (200), and (220) planes and show the presence of NiO. After reduction, a new diffraction peak arises at 44.57°, 51.76°, and 76.43°. JCPDS No. 04-0850[24–26] identifies this new peak as Ni, and it corresponds to the (111), (200), and (222) planes.

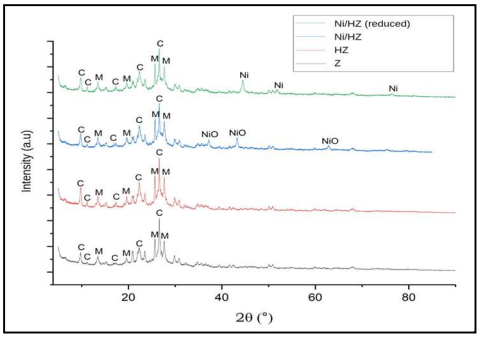

Fig.-1: Diffractogram of Natural Zeolite Before and After Impregnation

Zeolites that have been dedicated exhibit increased crystallinity but no change in crystal phase.[11,15] Desilication with NaOH 0.1 M reduces contaminants by removing amorphous particles surrounding the crystal. According to Zhao and Zhou[27], the NaOH content had a significant impact on the crystallinity of HZSM-5. Activating HZSM-5 with 0.1 M NaOH gave 93.97% crystallinity, which was not too different from the parent HZSM-5 (100%). This suggests that the crystal structure was not affected by 0.1 M NaOH. A rise in crystallite size from 30.53 nm to 40.85 nm corroborated the increase in crystallinity. The Debye-Scherrer equation was used to determine the size of the crystallite.

Table-2: SAA Analysis Results

Sample	BET Surface Area[a] (m^2/g)	S_{micro}[b] (m^2/g)	S_{meso}[c] (m^2/g)	Total Pore Volume[d] (cm^3/g)	Micropore Volume[e] (cm^3/g)	Mesopore Volume[f] (cm^3/g)	Pore Diameter (nm)
Z	34.8552	11.111	23.7442	0.078365	0.005723	0.072642	8.99319
HZ	53.0694	35.113	17.9564	0.108231	0.017990	0.090241	6.01817
Ni/HZ	21.4167	4.6900	16.7267	0.077149	0.002389	0.07476	14.4092

a. Multipoint BET; b. t-plot micropore surface area; c. $S_{meso} = S_{BET} - S_{micro;}$ d. Total pore volume at P/Po 0,99; e.t-plot micropore volume; f. $V_{meso} = V_{total} - V_{micro}$

Table-2 provides a summary of the N_2 adsorption-desorption properties. Desilication causes an increase in specific surface area[9], from 43.8552 to 53.0694 m^2/g. The increase in surface area indicates that the desilication has succeeded in removing impurities from the zeolite surface 11. NaOH desilication causes a decrease in pore size, from 8.99319 to 6.01817 nm, and an increase in pore volume, from 0.078365 to 0.108231 cm^3/g. This is due to the appearance of small pores caused by the release of the mineral

components that make up the zeolite. The loose component is indicated as amorphous Si. According to the results of the XRD analysis, the amorphous Si has low crystallinity, so it can dissolve in NaOH and increase the crystallinity. When Ni is added, the surface area drops from 53.0694 m^2/g to 21.4167 m^2/g. This is because the metal blocks the pores in the zeolite[28]. This means that there is less interaction between the adsorbate (N_2) and the zeolite.

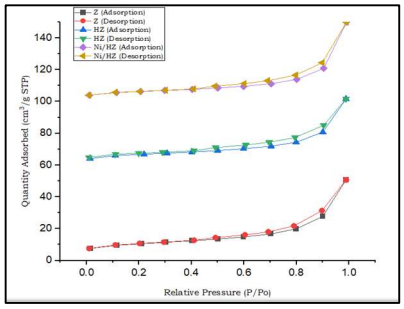

Fig.-2: Adsorption-Desorption Isotherm

The nitrogen adsorption-desorption isotherms are displayed in Fig.-2. The isothermal pattern in all samples is the same, displaying a hybrid form of type I and IV isotherms. The presence of micropores is indicated by very low adsorption at P/Po < 0.1 and a minor increase in adsorption between 0.1 < P/Po < 0.8. When P/Po > 0.8, adsorption goes up a lot, which suggests the formation of a hierarchical porous system that mixes microporous and mesoporous materials.[29] According to the IUPAC classification, the presence of a hysteresis loop at P/Po > 0.45 indicates the existence of mesoporous (2-50 nm) materials with type IV adsorption-desorption isotherm. This is consistent with Table-2's pore size data, which indicates that the sample's pore size is between 6 and 14 nm. Since HZ's hysteresis loop is broader than Z's, it contains a greater number of mesoporous gaps.[30]

The Effect of Variation in Adsorption Times on the Adsorption Capacity of H_2

The hydrogen uptake is measured at room temperature, 1 atm pressure, and varied adsorption times of 30, 45, 60, 75, and 90 minutes. This is done to find the best amount of time for adsorption, which is shown in Table-3.

Table-3: H_2 Adsorption Capacity Results from Variations in Adsorption Time

Sample	Temperature (T), °C	Pressure (P), atm	Time (t), (min)	Sample mass (g)	Mol H_2 (mmol)	H_2 adsorption capacity (mmol/g)	H_2 adsorption capacity (wt.%)
HZ	25	1	30	0.055	0.0480	0.8724	0.1745
	25	1	45	0.0511	0.0925	1.8102	0.3620
	25	1	60	0.0574	0.2188	3.8112	0.7624
	25	1	75	0.0524	0.0612	1.1673	0.2333
	25	1	90	0.0575	0.0518	0.9003	0.1802

The results in Table-3 show that the highest H_2 adsorption capacity is found at the adsorption time of 60 minutes, which is 3.8112 mmol/g (0.7624 wt.%). H_2 adsorption capacity continued to increase from 30 to 60 minutes, then decreased from 75 to 90 minutes. Figure-3 shows a graph of the adsorption pattern on HZB. Figure-4 shows the mechanism of H_2 adsorption on HZB. The adsorption step begins with a sharp increase in adsorption at the 25th minute, which is illustrated in Fig.-4 (a). After the 25th minute, the adsorption capacity will increase slowly and form a monolayer on the sample surface until the 45th minute, which is illustrated in Fig.-4 (b). H_2 will form a multilayer until it reaches a constant at 60-70 minutes due to the decrease in the empty active site because it has been filled with adsorbate (H_2), which is illustrated in Fig.- 4 (c). When it reaches a constant, H_2 will reach a saturation state. This situation causes the adsorbate to be released from the HZB surface, resulting in a decrease in adsorption capacity at 75 to 90 minutes.[31]

Comparison of H_2 Adsorption Capacity Between HZ and Ni/HZ

H_2 adsorption capacity is measured at room temperature and 1 atm pressure with an adsorption time of 60 minutes for HZ and Ni/HZ. This is done to compare the H_2 adsorption capacity between HZ and Ni/HZ, as well as study the effect of Ni metal on adsorption capacity, the results of which are presented in Table-4.

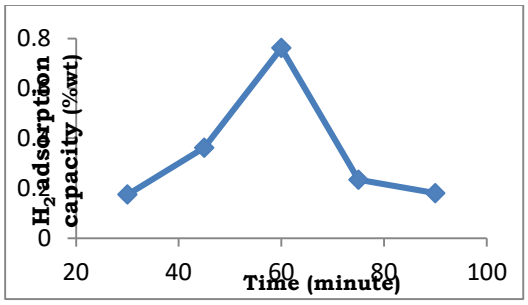

Fig.-3: Adsorption Pattern on HZ

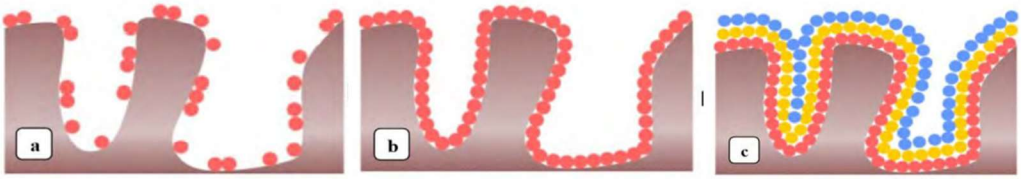

Fig.-4: Mechanism of H_2 Adsorption on Zeolite [31]

Table-4: Comparison of H_2 Adsorption Capacity Between HZ and Ni/HZ

Sample	Temperature (T), °C	Pressure (P), atm	Time (t), (min)	Sample mass (g)	Mol H_2 (mmol)	H_2 adsorption capacity (mmol/g)	H_2 adsorption capacity (wt.%)
HZ	25	1	60	0.0574	0.2188	3.8112	0.7624
Ni/HZ	25	1	60	0.0541	0.0380	0.7020	0.1405

Table-4 shows that HZ has a higher adsorption capacity than Ni/HZ. The addition of Ni metal to HZ did not increase the adsorption capacity but decreased it from 3.8112 mmol/g (0.7624 wt.%) to 0.7020 mmol/g (0.1405 wt.%). This is supported by a decrease in specific surface area and micropore area, as well as an increase in pore size in Table-2. The decrease in surface area occurs due to blocking or agglomeration, namely the blockage of the micropores by Ni metal. The increase in pore diameter also causes a decrease in adsorption capacity because the narrower pore conditions allow interactions between the pore walls and H_2 molecules to occur. [32-33] Ediati *et al*. (2017) reported that impregnation of 5% Ni on ZTC decreases the H_2 adsorption capacity from 2.124 to 0.331 wt.%. However, the more Ni loaded on ZTC, the more Ni loaded on ZTC, the more effect it had on the H_2 adsorption capacity.[30] Nishihara *et al.* (2009) reported that the addition of active metal (Pt) to ZTC can increase the H_2 adsorption capacity from 0.87 to 0.95 wt.%. [34] Through a spillover process, active metals like Pt, Pd, and Ni allow H_2 to be absorbed. The hydrogen spillover effect (HSPE) is what happens when active hydrogen atoms form in one phase (the metal surface) and move to a different phase (the support phase).[35] In the spillover mechanism, the H atoms move to the surface of the zeolite because the H^2 molecules stick to the metal surface in a way that does not bind them together.[34] Because of the Kubas contact and the oxidative strength of the metal, H_2 molecules stick to the metal surface without joining together.[36] The hydrogen atoms' (H-H) bonds become unstable due to the spillover effect, making it easier for the H-H bonds to break and release H atoms. More H atoms will enter the support pore than H_2 molecules, leading to more adsorption.[30] Figure-5 shows a breakdown of the spillover mechanism.

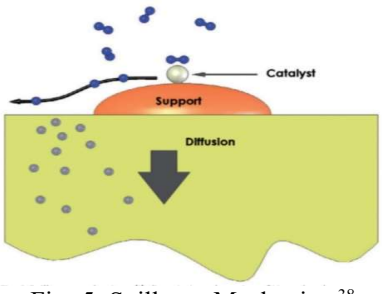

Fig.-5: Spillover Mechanism[38]

The H_2 molecules are adsorbed dissociative, the H atoms move to the support, and the H atoms spread out over most of the support.[37] According to the explanation above, the adsorption capacity of H_2 is not necessarily increased by adding active metal. The amount of H_2 that can be adsorbed depends on numerous parameters. The metal dispersion impacts the spillover effect, metal content, and pore texture. More evenly distributed metal on the support will have a higher adsorption capability.[39]

CONCLUSION

The desilication method using NaOH successfully modified Bogor natural zeolite into a hierarchical zeolite. The characterization using PSA revealed that milling can reduce particle size by up to 2 times the initial size. The XRD characterization confirmed that Bogor zeolite exhibited the mordenite and clinoptilolite frameworks on zeolite. Desilication in zeolite did not change the crystalline phase but could increase the crystallinity of the zeolite. The results of N_2 adsorption showed that desilication can increase the specific surface area. The largest H_2 adsorption capacity was found at an adsorption time of 60 min, which was 0.7624 wt.%. When Ni metal was added to HZ, the ability to absorb water dropped from 0.7624 wt.% to 0.1405 wt.%. This was due to a drop in the specific surface area and micropore area and an increase in the size of the pores.

ACKNOWLEDGEMENTS

The authors would like to thank the National research and Innovation Agency-BRIN for fundingthis work and all the facilities.

CONFLICT OF INTERESTS

The authors declare that there is no conflict of interests.

AUTHOR CONTRIBUTIONS

All the authors contributed significantly to this manuscript, participated in reviewing/editing, and approved the final draft for publication. The research profile of the authors can be verified from their ORCID IDs, given below:

Silvester Tursiloadi https://orcid.org/0000-0002-0642-6403
Aan Wahyuni https://orcid.org/0009-0009-5396-208X
Lenny Marlinda https://orcid.org/0000-0001-6961-3815
Muhammad Safaat https://orcid.org/0000-0003-0487-8868
Latifa Hauli https://orcid.org/0000-0003-2307-9789
Wiyanti Fransisca Manulang https://orcid.org/0000-0002-8265-0976
Amalia Kurnia Amin https://orcid.org/0000-0001-9409-480X
Deni Shidqi Khaerudini https://orcid.org/0000-0001-7171-8966
Muhammad Al Muttaqii https://orcid.org/0000-0001-5000-3478

REFERENCES

1. R. Rimbawati, C. Cholish, W. A. L. Tanjung, and M. A. R. Effendy, *CIRCUIT: Jurnal Ilmiah Pendidikan Teknik Elektro*, **5(1)**, 65(2021), https://doi.org/10.22373/crc.v5i1.8276
2. A. Kumar, S. Kaushal, S. A. Saraf, and J. S. Singh, *Frontiers In Bioscience, Landmark*, **23**, 1789(2018), https://doi.org/10.2741/4673
3. N. Valentino, Z. D. Hastuti, and A. Wibowo, *Jurnal Energi Dan Lingkungan (Enerlink)*, **13(2)**, 43(2017), https://doi.org/10.29122/elk.v13i2.4263
4. J. Chi and H. Yu, *Chinese Journal of Catalysis*, **39(3)**, 390(2018), https://doi.org/10.1016/S1872-2067(17)62949-8
5. S. I. Khasanah and N. Riveri Sesunan, *Jurnal Energi dan Manufaktur*, **12(2)**, 87(2019), https://doi.org/10.24843/JEM.2019.v12.i02.p07

6. F. Budi Pratama and Widyastuti, *Jurnal Teknik ITS*, **1**, 97(2012), https://doi.org/10.12962/j23373539.v1i1.823
7. J. Kolata and A. Martin, *Jom FTTEKNIK*, **1(2)**, 1(2014).
8. F. Rozi Z, A. Martin, and Nasruddin, *Jurnal Online Mahasiswa Fakultas Teknik*, **1(2)**, 1(2014).
9. A. Irawan, Y. Bindar, T. Kurniawan, H. Alwan, Rosid, and N. A. Fauziah, *Journal of Engineering and Technology Sciences*, **53 (3)**, 210308(2021), https://doi.org/10.5614/j.eng.technol.sci.2021.53.3.8
10. Liao X, Zhang Y, Guo J, Zhao L, Hill M, Jiang Z, Zhao Y, *Catalysts*, **7(9)**, 272(2017), https://doi.org/10.3390/catal7090272
11. D. Kurniawati, S. Tursiloadi, O. Arutanti, and M. Safaat, *Iranian Journal of Catalysis*, **11(3)**, 295(2021).
12. S.Tursiloadi, F. Afiyah, D. S. Khaerudini, M. Safaat, K. C. Sembiring, M. Al Muttaqii and S. Priatmoko, *ARPN Journal of Engineering and Applied Sciences*, **17(1)**, 58(2022).
13. M. Nasir, P. Ratnasari, D. N. F. Islam, and A. Shofyani, *Eksakta*, **18 (2)**, 200(2017), https://doi.org/10.24036/eksakta/vol18-iss02/78
14. N. P. Diantariani, I. Kartini, A. Kuncaka, and E. T. Wahyuni, *Rasayan Journal of Chemistry*, **13(1)**, 747(2020), https://doi.org/10.31788/RJC.2020.1315597
15. Y. K. Krisnandi, I. Mahmuda, D. U. C. Rahayu, and R. Sihombing, *Journal of Physics: Conference Series*, **1095(1)**, 18(2018), https://doi.org/10.1088/1742-6596/1095/1/012044
16. S. Li, S. Huang, K. Cai, Y. Li, J. Lv, and X. Ma, *Chinese Journal of Chemical Engineering*, **41**, 350(2022), https://doi.org/10.1016/j.cjche.2021.11.019
17. L. Patrylak, M. Krylova, and O. Pertko, *Chemistry & Chemical Technology*, **14(2)**, 234(2020), https://doi.org/10.23939/chcht14.02.234
18. M. Al Muttaqii, M. Amin, E. Prasetyo, R. Alviany, and L. Marlinda, *IOP Conference Series Earth and Environmental Science*, **926** ,012083(2021), https://doi.org/10.1088/1755-1315/926/1/012083
19. Aziz, R. A., Fauzi, N. F. N., Salleh, M. N., and Saleh, M, *IOP Conference Series Earth and Environmental Science*, **765**, 012028(2021), https://doi.org/10.1088/1755-1315/765/1/012028
20. Miądlicki, P., Wróblewska, A., Kiełbasa, K., Koren, Z. C., and Michalkiewicz, *Microporous and Mesoporous Materials*, **324**, 111266 (2021), https://doi.org/ 10.1016/j.micromeso.2021.111266
21. J. L. Sihombing, S. Gea, A. N. Pulungan, H. Agusnar, B. Wirjosentono, and Y. A. Hutapea, *AIP Conference Proceedings*, **2049**, 020062 (2018), https://doi.org/10.1063/1.5082467
22. A. A. Ahmed, M. R. Hashim, and M. Rashid, *AIP Conference Proceedings,* **2068**, 020076(2019), https://doi.org/10.1063/1.5089375
23. Srivastava and P. C. Srivastava, *Bulletin of Materials Science*, **33(6)**, 653(2010), https://doi.org/10.1007/s12034-011-0142-0
24. J. Huang, F. Li, B. Liu, and P. Zhang, *Materials (Basel)*, **13(3)**, 744(2020), https://doi.org/10.3390%2Fma13030744
25. L. K. P. M. M. Krylova and O. P. P. Yu, *Journal of Porous Materials*, **26**, 861(2019), https://doi.org/10.1007/s10934-018-0685-1
26. Teng, C., He, J., Zhu, L. *et al.*, *Nanoscale Research Letters,* **10**, 384(2015), https://doi.org/10.1186/s11671-015-1088-8
27. Y. Zhao and T. G. Y. W. Y. Zhou, Reaction Kinetics, *Mechanism and Catalysis*, **125**, 1085(2018). https://doi.org/10.1007/s11144-018-1426-9
28. S. Sumari, F. Fajaroh, ida bagus Suryadharma, A. Santoso, and A. Budianto, *IOP Conference Series: Materials Science and Engineering*, **515**, 0120752019(2019),https://doi.org/10.1088/1757-899X/515/1/012075
29. Silva, B. J. B., Sousa, L. V., Sarmento, L. R. A., Carvalho, R. P., Quintela, P. H. L., Pacheco, J. G. A., … Silva, A. O. S. *Microporous and Mesoporous Materials,* **290**, 109647(2019), https://doi.org/10.1016/j.micromeso.2019.109647
30. R. Ediati, A. Mukminin, and N. Widiastuti, *Indonesian Journal of Chemistry*, **17(1)**, 30(2017), https://doi.org/10.22146/ijc.23563
31. F. C. Suci. Thesis, Department of Chemistry, Sepuluh Nopember Institute of Technology, Surabaya, Indonesia (2015).

32. Konwar, R. J., and De, M. *Microporous and Mesoporous Materials,* **175**, 16(2013), https://doi.org/10.1016/j.micromeso.2013.03.014
33. Konwar, R. J., & De, M. *International Journal of Energy Research,* **39(2)**, 223(2014), https://doi.org/10.1002/er.3232
34. Nishihara, H., Hou, P.-X., Li, L.-X., Ito, M., Uchiyama, M., Kaburagi, T., … Kyotani, T. *The Journal of Physical Chemistry C,* **113(8)**, 3189(2009), https://doi.org/10.1021/jp808890x
35. H. Shen, H. Li, Z. Yang, and C. Li, *Green Energy and Environment*, **7(6)**, 1161(2022), https://doi.org/10.1016/j.gee.2022.01.013
36. S. Lee, J. Lee, Y. Kim, J. Kim, and K. Lee, *Processes*, **10(2)**, 304(2022), https://doi.org/10.3390/pr10020304
37. J. Lyu, V. Kudiiarov, and A. Lider, *Nanomaterials*, **10(2)**, 255(2020), https://doi.org/10.3390/nano10020255
38. B. D. Adams and A. Chen, *Materials Today*, **14(6)**, 282(2011), https://doi.org/10.1016/S1369-7021(11)70143-2
39. Zhao, W., Luo, L., Chen, T., Li, Z., Zhang, Z., Wang, H., … Fan, M. *Composites Part B: Engineering*, **161**, 464(2019), https://doi.org/10.1016/j.compositesb.2018.12.122

[RJC-8306/2023]